Int. J. Electrochem. Sci., 5 **(2010)** 459 - 477

International Journal of ELECTROCHEMICAL SCIENCE
www.electrochemsci.org

Solvent Effect on the Reduction Potential of Anthraquinones Derivatives. The Experimental and Computational Studies

Davood Ajloo[*], *Behnaz Yoonesi, Ahmad Soleymanpour*

School of Chemistry, Damghan University of Basic Science, Damghan, Iran
[*]E-mail: ajloo@dubs.ac.ir

Received: 24 November 2009 / *Accepted:* 15 April 2010 / *Published:* 30 April 2010

Electrochemical behavior of some anthraquinone (Aq) derivatives were investigated in acetonitrile (AN), N,N-dimethyl formamide (DMF) and dimethylsulfoxide (DMSO) by cyclic voltammetry (CV), quantum mechanics and statistical methods. A reasonable correlation between the computational and experimental standard reduction potential (E^o) for electron transfer was obtained. It was concluded that the first step reduction potential, E_1^o in acetonitrile, increases with hydrogen bonding, aromaticity and HOMO energy and decreases with size and polarity of anthraquinone. Trend of average values for E_1^o in three solvents is AN < DMSO < DMF, while the trend of E_2^o is inversely. The E_1^o values increase with polarity, dielectric constant, molecular size and hydrogen bonding of solvent and this trend is reverse in the case of E_2^o values. Difference in trend of reduction potential is related to solute-solvent and solvent interactions. Solvent effect in the explicit model presents better correlation with experimental E^o.

Keywords: Anthraquinones, Solvent effect, Cyclic voltammetry, Quantitative structure-property relationship (QSPR), Self consistent reaction field.

1. INTRODUCTION

9,10-anthraquinones (AQs) as the largest group of naturally occurring quinones are of fundamental importance both in industry and medicine [1-4]. Therefore, study of the electrochemical behavior of different anthraquinone derivatives in non-aqueous aprotic solvents has received considerable attention during the past two decades [5,6].

Solvent effects on the redox properties of radicals and radical ions have been a subject of considerable interest [7-12]. The solvent effect on the redox potential is interpreted based on interaction between solute and solvent such as; solute-solvent hydrogen bonding, Lewis acid-base interactions and solute-solvent π-stacking of ring systems. The solvent effect on different systems was

studied by several methods. The multi parameter equation of Kamlet, Abboud, and Taft for correlating a physicochemical quantity with solvent properties has been validated extensively with a large number of systems [13].

Solvent effect also was studied by self consistent reaction field (SCRF) quantum mechanics. The polarized continuum model (PCM) [14-16] is a more detailed approach that accounts explicitly for the molecular shape of the solute cavity, and also accounts for certain nonelectrostatic terms such as the cavitation energy and solute-solvent dispersion interaction.

Relative redox potentials for substituted benzoquinones were calculated to an accuracy of 50 mV at the AM1 or PM3 level using continuum solvation model (COSMO) [17]. Electrode potentials of some of benzoquinones and naphtoquiniones were calculated using ab initio and AM1 methods. The effect of individual contributions from electrostatic, cavity and dispersion interactions were analyzed for polar and nonpolar molecules. Comparison of the AM1 calculated potentials with the AM1-COSMO results shows the superiority of the SCRF model and importance of the inclusion of the cavity and dispersion terms [18]. Electrode potentials were computed theoretically for quinones by using a combination of statistical and quantum mechanics [19]. Moreover, electrode potential of benzoquinones in aqueous solution have been calculated using a thermodynamic cycle approach that includes accurate gas-phase ab initio calculation of differences in free energies of hydration using the free-energy perturbation method [20].

The one-electron reduction potential of the radical cations of thioanisole, benzyl methyl sulfide and 2-hydroxyethyl benzyl sulfide in different solvents was investigated by cyclic voltammetry. The redox potential is strongly influenced by the nature of the solvent and the solvent sensitivity increases with charge localization. The results have been used to evaluate solvent effects in view of the Kamlet-Taft relationship [21].

The electrochemical behavior of 33 derivatives 9,10 anthraquionones were studied in acetonitrile solution by cyclic voltammetery [22-25]. Some properties such as peak potentials and half-wave reduction potentials were determined from recorded cyclic voltammograms. Semi-empirical PM3 and DFT methods at the level of B3LYP have been used to compute the redox potentials. But they didn't calculate the reduction potential for second step. So in our studies, the second reduction potential as well as solvent effect are calculated and interpreted based on Kamlet-Taft relationship.

We recently applied quantitative structure-property relationship (QSPR) and principal component analysis (PCA) for prediction of thermal stability of polymers and inhibition constant of some nucleoside and non-nucleosides compounds [26, 27]. The aim of this work is study of the substituent and solvent effect on the reduction potential for antraquinone derivatives. Reduction potential for the first and second steps and free energy of solvation for neutral, radical anion and dianion anthraquinones are compared. The effects of substituents and solvent on the reduction potentials are interpreted based on polarity, charge, size, shape, hydrogen bond, aromaticity and dielectric constant of solute and solvent. Experimental cyclic voltammetry and computational quantum calculation results are compared and ability of quantum mechanics in estimation of reduction potential are tested.

2. EXPERIMENTAL PART

2.1. Chemicals

Acetonitrile (AN), dimethylformamide (DMF), dimethylsulfoxide (DMSO) and tetrabutylammonium perchlorate (TBAP) were purchased from Fluka chemical Co. Some of 9,10-anthraquinone derivatives such as 1,8-dihidroxy 1,4-dihydroxyl, 1-hydroxy, 1-amino and 2-amino anthraquinones were of the highest purity, available from Merck chemical company and used as received. Other anthraquinones i.e. 1-methoxy, 1,4-dimethoxy, 1,8-dimethoxy, and 2-hydroxy derivatives were synthesized as literature [28] and used after recrystalization and vacuum drying. Structure of the anthraquinone derivatives were shown in Scheme 1.

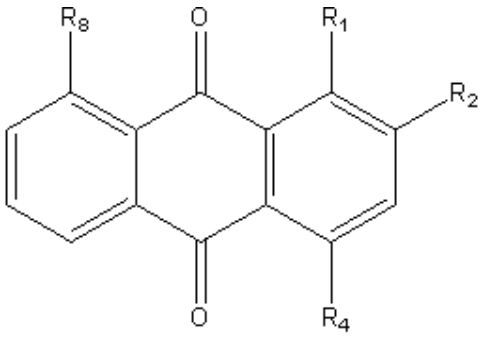

Aq	R_1	R_2	R_4	R_8
Aq1	**H**	**H**	**H**	**H**
Aq2	**OH**	**H**	**H**	**H**
Aq3	**OCH_3**	**H**	**H**	**H**
Aq4	**NH_2**	**H**	**H**	**H**
Aq5	**H**	**OH**	**H**	**H**
Aq6	**H**	**NH_2**	**H**	**H**
Aq7	**OH**	**H**	**OH**	**H**
Aq8	**OH**	**H**	**H**	**OH**
Aq9	**OCH_3**	**H**	**OCH_3**	**H**
Aq10	**OCH_3**	**H**	**H**	**OCH_3**

Scheme 1. Structural features of the anthraquoinone derivatives.

2.2. Methods

2.2.1 Cyclic voltammetry

All voltammograms were recorded with a three electrode system utilizing an Autolab multipurpose electroanalyzer model PGSTAT. The reference electrode Ag/AgCl (satd.), 0.1 M in actonitrile in a separate compartment with a dense ceramic in bottom, was directly immersed in the

reaction cell. The working electrode was a glassy carbon (Metrohm, 2 mm diameter). The counter electrode was a platinum rode. The working GC electrode was polished with alumina powder (0.05 μm) followed by washing with water and acetone before each cyclic voltammogram. Cyclic voltammograms were recorded by the scan rates varied from 20 mVs^{-1} to 1000 mVs^{-1} by potential cycling between 0 and -1800 mV. The electrochemical measurements were carried out at a thermostated temperature of 25.0 ± 0.1 ℃. In all experiments, the test solutions were dearated by stream of N_2 gas passing the solution for at least 15 min.

2.2.2. Quantum mechanics calculation

The molecular structures of anthraquinones derivatives were drawn by Hyperchem 7.0 software. All structures were optimized by PM3 semi-empirical method [29] and subsequently by ab initio 6-31G basis set at 298 K by Gaussian 98 program [30]. The optimized structures of neutral and anion species were used for the further calculations such as frequency and solvation free energy calculations.

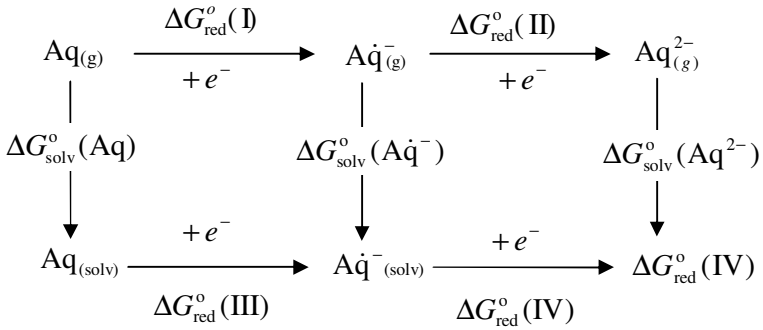

$$1/2\,H_2 \xrightarrow{\Delta G^{o}_{ox}} H^{+}_{aq} + e^{-}$$

$$\Delta G^{o}_{red}(Aq^{\cdot -}/Aq \text{ vs. SHE}) = \Delta G^{o}_{red} + \Delta G^{o}_{ox}$$

Scheme 2. Thermodynamic cycle for computing the reduction potential by *ab initio* method.

Solvation free energies were calculated as single points on the 6-31G and default parameters in the polarizable continuum model (PCM), implemented in Gaussian 98 for a range of charged and uncharged species. In the PCM model, the solvation energy is partitioned into four components including electrostatic (ΔG_{elec}), cavity (ΔG_{cav}), dispersion (ΔG_{disp}) and repulsion energies (ΔG_{rep}). The last three terms form non-electrostatic interactions between solute and solvent.

We adopted a common thermodynamic cycle strategy to relate standard reduction potentials in non-aqueous solution to electron affinities in the gas-phase and solvation free energies (ΔG_{solv}) (Scheme 2) [31]. The free energy cycle shown in Scheme 2 was used to compute the free energy change for the reaction in solution. Using the Nernst equation, $\Delta G^{o}_{red} = -nFE^{o}$, reduction potential can

be calculated, where n is the number of electrons transferred and F is Faraday's constant. Using this cycle, the standard reduction potentials of $Aq/A\dot{q}^-$ and $A\dot{q}^-/Aq^{2-}$ couples in the three solvents can be determined as Scheme 2. The calculation of the change in free energy, including solvation, yields ΔG^o_{red}. The reduction potential determined in this manner is an absolute reduction potential, because it has not been referenced to a standard electrode. By subtracting 4.43 eV, the absolute reduction potential estimated for NHE [32].

The calculated reduction potentials were obtained for the standard conditions of 298 K, 1 atm and 1 M H^+ vs. NHE. The Gibbs free energies and standard reduction potential can be obtained as following equations:

$$\Delta G^{o}_{red}(III) = \Delta G^{o}_{g}(I) + \Delta G^{o}_{solv}(A\dot{q}^-) - \Delta G^{o}_{solv}(Aq) \quad (1a)$$

$$\Delta G^{o}_{red}(IV) = \Delta G^{o}_{g}(II) + \Delta G^{o}_{solv}(Aq^{2-}) - \Delta G^{o}_{solv}(A\dot{q}^-) \quad (1b)$$

$$\Delta G^{o}_{red} = -nFE^{o} \quad (2)$$

Interaction energy between anthraquinones and solvent molecules were explicitly calculated by MM^+ molecular mechanics in Hyperchem7.

2.2.3. Statistical study

The molecular descriptors were calculated by Hyperchem 7.0 and Dragon 3.0 softwares. Correlation between experimental parameter (E^o) and cited descriptors were obtained by Pearson correlation in SPSS. Then, an equation representing relation between the experimental values and molecular descriptors were obtained using multiple linear regression (MLR). The descriptors with similar effects were reduced into the new categories or principal components (PCs) by factor analysis. Finally, correlation between experimental values and these PCs were obtained.

3. RESULTS AND DISCUSSION

3.1. Cyclic voltammetry results

Cyclic voltammetry of anthraquinones Aq1-Aq10 at GC electrode as working electrode were recorded in AN, DMF and DMSO solvents with varying scan rates (20-1000 mVs^{-1}) between 0 and -1800 mV. Cyclic voltammograms were recorded in 1 mM of the anthraquinones with 100 mM TBAP. The obtained data were shown in Table 1 and some typical voltammograms for scan rate 100 mV/s were also shown in Figure 1. The cyclic voltammograms of anthraquinnone derivatives at GC electrode in all scan rates showed two successive cathodic and anodic peaks. The cathodic peak currents vary linearly with concentration of anthraquinone.

The cathodic (I_{pc}) and anodic (I_{pa}) peak currents vary linearly with square root of scan rate at various potential scan rates (v). Results of Table 1 shows that the I_p vs. $v^{1/2}$ is quite linear (figure not shown) and therefore the current function, $I_p/v^{1/2}$ is constant. All corresponding waves were found to be diffusion controlled. The ratio of anodic to cathodic peak currents is constant (Table 1) and is about one "for scan rates between 20-1000 mVs^{-1}" which indicates the stability of anion radical and dianion in the experimental condition. The values of peak separation (ΔE_p) and reduction potential (E^o) for Aq1-Aq10 compounds were also evaluated and listed in Table 1.

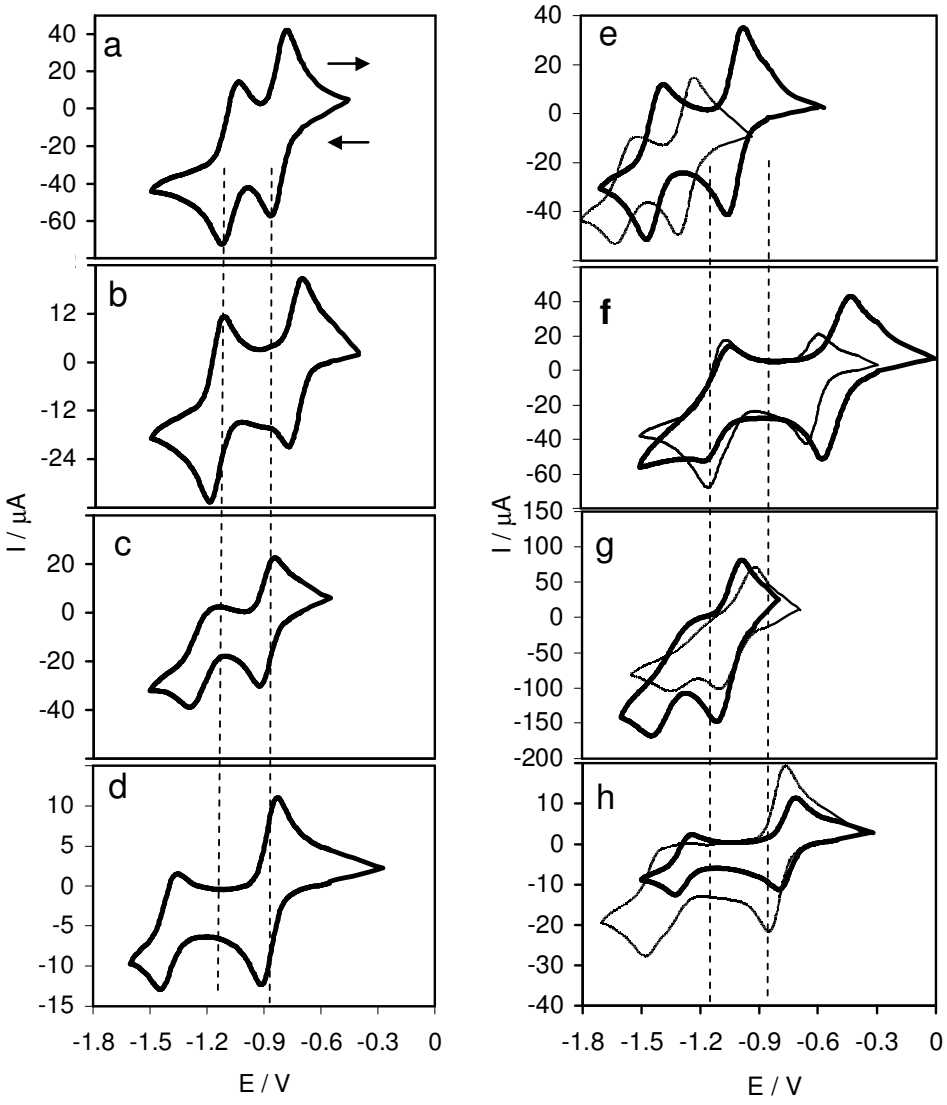

Figure 1. Cyclic voltammograms for 1.0 mM a) Anthraquinone (Aq1), b) 1-hydroxy (Aq2), c) 1-methoxy (Aq3), d) 1-amino anthraquinones (Aq4), and comparison between e) 2-hydroxy (Aq5, thin line) and 2-amino (Aq6, bold line) (f) 1,4-dihydroxy (Aq7, thin line) and 1,8-dihydroxy (Aq8, bold line), g) 1,4-dimethoxy (Aq7, thin line) and 1,8-dimethoxy (Aq8, bold line) in acetonitrile and h) Aq1 in DMF (thin line) and in DMSO (bold line) at scan rates 100 mVs^{-1}.

Table 1. Cyclic voltammetry data for anthraquinones (Aq1-Aq10) in different solvents at scan rate 100 mV/s.

Aq	AN						DMSO						DMF					
	First wave			Second wave			First wave			Second wave			First wave			Second wave		
	E_1^o	ΔE_p	I_{pa}/I_{pc}	E_2^o	ΔE_p	I_{pa}/I_{pc}	E_1^o	ΔE_p	I_{pa}/I_{pc}	E_2^o	ΔE_p	I_{pa}/I_{pc}	E_1^o	ΔE_p	I_{pa}/I_{pc}	E_2^o	ΔE_p	I_{pa}/I_{pc}
Aq1	-0.823	0.082	0.99	-1.092	0.065	0.99	-0.760	0.074	0.99	-1.290	0.083	0.98	-0.809	0.091	0.99	-1.350	0.088	0.94
Aq2	-0.742	0.068	0.99	-0.956	0.075	0.99	-0.612	0.110	0.99	-1.113	0.071	0.99	-0.671	0.098	0.99	-1.040	0.195	0.92
Aq3	-0.972	0.075	0.99	-1.334	0.066	0.99	-0.871	0.096	0.98	-1.401	0.066	0.95	-0.891	0.092	0.98	-1.240	0.205	0.95
Aq4	-0.896	0.092	0.98	-1.212	0.147	0.95	-0.843	0.092	0.99	-1.357	0.093	0.98	-0.843	0.184	0.98	-1.257	0.195	0.93
Aq5	-1.204	0.080	0.99	-1.841	0.117	0.97	-1.117	0.078	0.99	-1.627	0.071	0.99	-1.283	0.192	0.98	-1.559	0.332	0.96
Aq6	-1.023	0.082	0.99	-1.433	0.076	0.99	-0.925	0.096	0.98	-1.420	0.149	0.94	-0.932	0.134	0.98	-1.318	0.218	0.92
Aq7	-0.644	0.064	0.99	-0.789	0.094	0.96	-0.514	0.098	0.99	-1.031	0.078	0.99	-0.535	0.078	0.99	-1.080	0.078	0.94
Aq8	-0.531	0.094	0.99	-0.572	0.124	0.96	-0.520	0.146	0.98	-1.035	0.107	0.95	-0.532	0.126	0.99	-1.044	0.124	0.91
Aq9	-1.011	0.130	0.98	-1.407	0.159	0.95	-0.915	0.121	0.98	-1.416	0.149	0.95	-0.945	0.181	0.98	-1.325	0.232	0.91
Aq10	-1.053	0.106	0.98	-1.474	0.108	0.96	-0.940	0.110	0.99	-1.455	0.071	0.99	-0.971	0.122	0.98	-1.346	0.238	0.90
Average	-0.889			-1.211			-0.802			-1.314			-0.841			-1.256		

Table 2. Calculated Gibbs free energy for two reduction steps of anthraquinones in the gas phase (atomic unit, a.u.) and different solvents (kcal mol^{-1}).

Aq	G_{gas}			ΔG_{solv}(AN)			ΔG_{solv} (DMSO)			ΔG_{solv} (DMF)		
	Aq	$Aq^{\bullet-}$	Aq^{2-}	Aq	$Aq^{\bullet-}$	Aq^{2-}	Aq	$Aq^{\bullet-}$	Aq^{2-}	Aq	$Aq^{\bullet-}$	Aq^{2-}
Aq1	-680.5	-680.6	-680.5	0.6	-39.0	-166.9	-3.7	-43.7	-172.5	-6.9	-51.2	-201.2
Aq2	-755.0	-755.0	-755.0	1.5	-37.3	-162.3	-3.1	-42.2	-168.1	-4.9	-48.1	-193.8
Aq3	-835.2	-835.3	-835.3	0.6	-39.9	-167.9	-4.1	-44.9	-173.8	-7.8	-53.1	-203.2
Aq4	-793.7	-793.8	-793.7	-0.1	-42.2	-170.2	-4.9	-47.5	-176.4	-9.29	-55.4	-207.2
Aq5	-1072.2	-1072.0	-1072.3	0.5	-40.4	-167.0	-4.1	-45.3	-172.8	-7.3	-55.7	-204.1
Aq6	-904.8	-904.3	-904.9	-0.7	-42.8	-171.0	-5.4	-46.8	-177.1	-9.8	-58.2	-205.6
Aq7	-616.9	-616.5	-616.8	2.2	-36.4	-160.8	-2.1	-41.5	-166.8	-3.0	-48.0	-190.2
Aq8	-487.4	-487.3	-487.3	-0.2	-42.0	-169.8	-5.1	-47.2	-176.1	-7.9	-56.5	-206.2
Aq9	-865.9	-865.9	-865.9	-1.4	-44.0	-173.3	-6.9	-49.9	-180.2	-11.9	-59.6	-211.8
Aq10	-906.9	-907.0	-907.0	-1.3	-45.8	-174.2	-6.7	-51.8	-181.2	-13.2	-62.6	-213.6
Average	-791.9	-791.8	-791.9	0.171	-41.2	-168.3	-4.6	-46.1	-174.5	-8.2	-54.8	-203.7

3.2. Computational quantum mechanics results

Following electrochemical studies of anthraquinones in three solvents AN, DMF and DMSO, the calculation of Gibbs free energy for ten anthraquinones in oxidized, reduced radical anion and dianions forms were carried out in the gas phase and the results were summarized in Table 2.

In order to evaluate the Gibbs free energy of anthraquinones for redox reaction, the corresponding solvation energies consisting electrostatic and non-electrostatic terms were computed

using the SCRF/PCM method and the resulting values were shown in Table 2. It is worth mentioning that the average solvation energies calculated for anionic anthraquinones are much larger than those of corresponding neutral anthraquinone derivatives, i.e. $Aq^{2-} > A\dot{q}^{-} > Aq$ (the last row of Table 2). This is obviously due to strong electrostatic interaction between the charged species and solvent molecules. Trend of negative free energies of solvation for three forms of anthraquinones in three solvents is AN < DMSO < DMF. This is due to polarity, size, hydrogen bond and dielectric constant of solvents. Reduction potentials were calculated by equation (2) and listed in Table 3. Correlation between experimental data; $E^o(\text{exp})$; and calculated data; $E^o(\text{cal})$; can be described as following equations.

$$\begin{aligned}
&E_1^o(\text{exp}) = 0.1083E_1^o(\text{cal}) - 0.7173 \quad R^2 = 0.990 \quad \text{AN}\\
&E_2^o(\text{exp}) = 0.1985E_2^o(\text{cal}) - 0.2296 \quad R^2 = 0.997 \quad \text{AN}\\
&E_1^o(\text{exp}) = 0.1044E_1^o(\text{cal}) - 0.6305 \quad R^2 = 0.949 \quad \text{DMSO}\\
&E_2^o(\text{exp}) = 0.1037E_2^o(\text{cal}) - 0.5564 \quad R^2 = 0.930 \quad \text{DMSO}\\
&E_1^o(\text{exp}) = 0.1154E_1^o(\text{cal}) - 0.6307 \quad R^2 = 0.945 \quad \text{DMF}\\
&E_2^o(\text{exp}) = 0.0789E_2^o(\text{cal}) - 0.5917 \quad R^2 = 0.827 \quad \text{DMF}
\end{aligned} \tag{3}$$

As seen from these equations, there are good correlation coefficients between experimental and calculated $E°$ values by equation (2).

Table 3. Quantum mechanics calculated values of E^o/ V for anthraquinone derivatives in three solvents.

Aq	E_1^o			E_2^o		
	AN	DMSO	DMF	AN	DMSO	DMF
Aq1	-0.752	-0.666	-0.692	-0.936	-1.171	-1.147
Aq5	-0.818	-0.726	-0.757	-1.099	-1.257	-1.206
Aq6	-0.947	-0.843	-0.888	-1.312	-1.368	-1.297
Aq7	-0.909	-0.810	-0.847	-1.209	-1.314	-1.259
Aq4	-1.252	-1.121	-1.208	-1.816	-1.631	-1.505
Aq8	-1.043	-0.927	-0.993	-1.478	-1.455	-1.358
Aq2	-0.657	-0.583	-0.606	-0.794	-1.099	-1.081
Aq3	-0.507	-0.444	-0.457	-0.570	-0.980	-1.008
Aq9	-0.996	-0.888	-0.940	-1.408	-1.418	-1.338
Aq10	-1.061	-0.948	-1.003	-1.473	-1.453	-1.363
Average	-0.894	-0.795	-0.839	-1.209	-1.314	-1.256

3.3. Substituent effect

3.3.1. Qualitative discussion

In water, the reduction of anthraquinones to corresponding hydroquinone usually occurs reversibly as a two-electron and two-proton transfer process [33,34]. However, as it is expected, the

electrochemistry of anthraquinones in non-aqueous aprotic solvents such as acetonitrile must differ significantly. In aprotic solvent, it can be written:

$$Aq + e \rightarrow A\dot{q}^{-} \quad (4a)$$

$$A\dot{q}^{-} + e \rightarrow Aq^{2-} \quad (4b)$$

The difference between anodic and cathodic peak potentials recorded by cyclic voltammetry in three solvents; AN, DMF and DMSO were given in Table 1. As seen from Table 1, the redox potentials of 9,10-anthraquinone molecules strongly depend on both the nature and position of the substituting groups on the anthraquinone. This is due to formation of hydrogen bonding between hydroxyl group and a neighboring carbonyl group of anthraquinones, that stabilizes the resulting radical intermediate, as well as varying resonance and inductive effects of different groups substituted on various positions of 9,10-anthraquinone.

Figures 1a-d show the voltamograms related to four anthraquinones derivatives (Aq1, Aq2, Aq3 and Aq4) which have H, OH, OCH_3 and NH_2 substituents, respectively at position 1. In order to compare the anthraquoinone better, we took the Aq1 as a reference and passed two vertical dashed lines through the two minima of the cathodic peak for Aq1. If the hydrogen of 9,10-anthraquinone (Aq1) is replaced by a hydroxyl group (Aq2), then the reduction potential of the first peak shifts to less negative (more positive) values as compare with Aq1 (Figure 1b). Thus, it has less negative E^{o} and higher tendency for reduction relative to hydrogen substituent. On the other hand, second cathotic peak was shifted to the left that shows radical anion has less tendency for converting to dianion derivative. While two CV peaks of OCH_3 (Figure 1c) were shifted to the left namely, it has less tendency to reduce due to electron donating nature of OCH_3. Cathodic peaks of anthraquinone with NH_2 group (Aq4) were shifted to the left more than H substituent and second cathodic peak even shifted more than OCH_3 and OH groups (Figure 1d). This is more probably because of higher electron donating of NH_2 relative to other groups.

Substitution at position 2 reveals some shift in the peak potentials, either positive or negative depend on the nature of substituting group. However, the extent of shift in potential is not as significant as that observed for the substitution at position 1 of 9,10-anthraquinone. Replacement of hydrogen atoms by OH and NH_2 at position 2 (Figure 1e) gives Aq5 (thin line) and Aq6 (bold line) derivatives, respectively. Both hydroxyl and amino groups shift the peaks to the left. These variations are higher in the NH_2 and OH group. The reason is that intramolecular hydrogen bonding at position 2 is less favorable than position 1 and so OH and NH_2 groups show inductive effect which appear as an electron donation in anthraquinone. In this electron donation, amine group is more effective than hydroxyl group.

Replacement of hydrogen atoms at positions 1,4 and 1,8 by two hydroxyl groups gives Aq7 and Aq8, respectively. Figure 1g shows that 1,4 (dashed line) and 1,8 dihydroxy (bold line) shift the peak to the right. Because increasing hydrogen boding in these two regions specially at 1,8 positions, also increases tendency for reduction .

Replacement of hydrogen atoms at positions 1,4 and 1,8 by two methoxy groups give Aq9 and Aq10 which results a shift in the first cathodic waves toward more negative potentials. The more

tendency for reduction of the anthraquinones Aq2, Aq4, Aq7 and Aq8, when compared with, Aq9 and Aq10, (Table 1),can be attributed to the intra-molecular H-bonding between the hydroxyl groups at position(s) 1, 4, 8 and the neighboring 9- and/or 10- carbonyl oxygen atoms. The hydrogen bond reduces the electron density on the carbonyl oxygen atoms(s) and thus increases the electrophilic nature of the aromatic system and stabilizes the semi-quinone anion radical formed during the charge transfer process [13].

Finally, effect of solvent on the CV voltammogram depicted that the first cathodic and anodic peaks of Aq1 in DMSO and DMF (Figure 1h) shifted to right and second cathodic and anodic shifted to left relative to Aq1 in acetonitile (Figure 1a).

Table 4. First standard reduction potentials, E_1^o, values in acetonitrile and their correlation with calculated values of molecular descriptors by Dragon 3.0 and Hyperchem 7.0.

Aq	E_1^o	**HOMA**	**AROM**	**HOMT**	**L/Bw**	**RGyr**	**ASP**	**Surface**	**Volume**	**Polar**	**Refract**	**ChargeO10**	**Dipole**	***E*HOMO**
Aq1	-0.742	0.81	0.94	9.66	2.5	4.90	0.39	306	640	25.0	66.01	-0.36	2.40	-7.2
Aq5	-0.823	0.75	0.95	9.50	2.3	4.12	0.37	287	689	25.6	67.62	-0.30	2.46	-7.5
Aq6	-0.972	0.70	0.91	8.45	2.3	5.37	0.36	358	731	26.7	70.56	-0.34	3.60	-10.8
Aq7	-0.896	0.70	0.94	8.20	2.4	4.61	0.38	331	674	25.6	67.61	-0.29	3.46	-9.7
Aq4	-1.204	0.60	0.87	7.19	3.1	5.77	0.45	402	796	28.3	75.07	-0.30	4.70	-12.8
Aq8	-1.023	0.69	0.9	8.26	3.1	5.45	0.45	364	745	27.1	71.54	-0.30	3.80	-10.2
Aq2	-0.644	0.85	0.97	9.80	1.8	4.33	0.31	292	628	24.5	64.54	-0.36	2.26	-5.4
Aq3	-0.531	0.86	0.97	11.40	2.1	4.30	0.34	274	630	24.0	64.65	-0.41	1.52	-3.6
Aq9	-1.011	0.73	0.92	8.01	2.7	5.20	0.41	336	763	27.7	74.08	-0.28	3.68	-11.2
Aq10	-1.053	0.69	0.87	8.50	2.8	5.12	0.42	375	752	28.1	74.08	-0.28	4.33	-11.5
$R(E_1^o)$[a]		**0.962**	**0.924**	**0.948**	**-0.842**	**-0.840**	**-0.837**	**-0.937**	**-0.956**	**-0.965**	**-0.943**	**-0815 or 0.815**	**-0.976**	**0.984**

[a] $R(E_1^o)$ is correlation coefficient between E_1^o in acetonitrile and descriptors

HOMA; Harmonic Oscillator Model of Aromaticity index
AROM; Aromaticity (trial)
HOMT; HOMA total (trial)
L/Bw; Length-to-breadth ratio
RGyr; Radius of gyration (mass weighted)
ASP; Asphericity
Surface; Accessible surface area
Volume; Volume
Polar; Polarizabilitry
Refract; Refractivity
ChargeO10; Charge on oxygen connected to carbon 10
Dipole; Dipole moment
***E*HOMO**; Highest occupied molecular orbital energy

3.3.2. Quantitative and statistical discussion

Molecular structures of all anthraquinones were optimized by HF/6-31G method. Then, molecular descriptors were calculated by Dragon 3.0 and Hyperchem 7.0. Definition of descriptors and

corresponding values were tabulated in Table 4. Correlation between reduction potential, E_1^o, in acetononitrile was obtained by Pearson method that implemented in the SPSS software (Table 4).

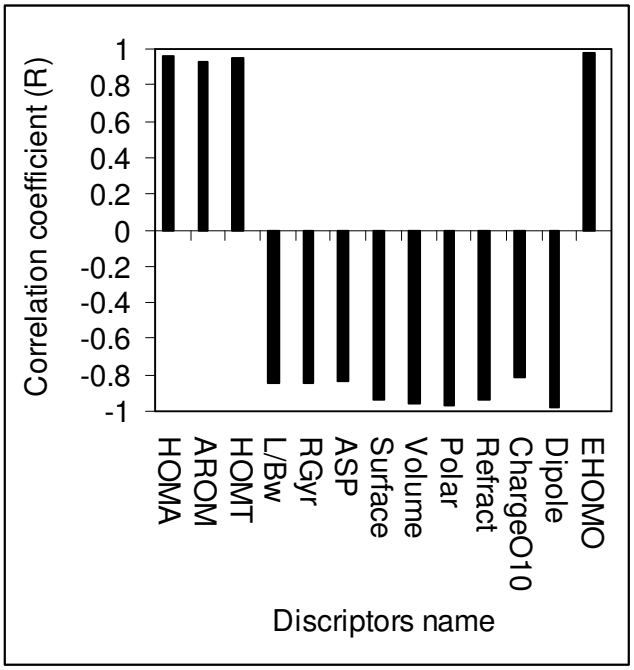

Figure 2. Bar line plot of correlation coefficient between experimental first reduction potential, E_1^o, in acetonitrile and molecular descriptors.

Correlation coefficients in the last two rows of Table 4 which also plotted in Figure 2, show that aromaticity descriptors; HOMA, AROM and HOMT and highest occupied molecular orbital energy, *E*HOMO have directly correlate to E_1^o and other descriptors have inversely correlated to this parameter. Reduction potential decreases by size dependent descriptors, such as volume, surface area, polarizability, number of atoms and number of functional groups. The MLR analysis by stepwise selection shows that E_1^o is correlated to *E*HOMO and volume as following:

$$E_1^o = (0.479 \pm 0.009)E\text{HOMO} - (0.0010 \pm 0.0001)Volume + (0.311 \pm 0.023) \quad (5)$$
$$R = 0.952,\ F = 211,\ n = 10$$

As it was discussed, some descriptors, such as size descriptors have common properties, so can be classified based on their inter-correlation. Therefore, principal component analysis (PCA) used to reduce the descriptors to several categories with similar properties. Results of PCA were summarized in Table 5. It was shown that size parameters such as volume, surface, radius of gyration (RGyr), and aromaticity (AROM) are only located in principal component 1 (PC1), while electronic descriptors in PC2 and shape descriptors such as length to breath ratio (L/Bw) and aspherosity (ASP) only locate in PC3. Thus, PC1, PC2 and PC3 have mostly size, electronic and shape properties, respectively. Some of

descriptors such as; HOMA, HOMT, polarizability, refractivity, dipole moment and *E*HOMO are simultaneously belong to size and electronic factor. Correlation between E° and three principal components are analyzed by MLR. The resulted equation depicts decreasing of E° values with size, shape and electronic factors, as following:

$$E_1^\circ = -(0.100 \pm 0.017)PC1 - (0.009 \pm 0.001)PC2 - (0.162 \pm 0.032)PC3 + (0.890 \pm 0.022) \quad (6)$$
$$R = 0.99,\ F = 114,\ n = 10$$

Table 5. Rotated component matrix for studied descriptors

Descriptor	Components		
	Size (PC1)	Electronic (PC2)	Shape (PC3)
HOMA	-0.627	-0.61	
AROM	-0.734		-0.503
HOMT	-0.615	-0.697	
L/Bw			0.83
RGyr	0.853		
ASP			0.837
Surface	0.825		
Volume	0.659	0.533	
Polar	0.655	0.57	
Refract	0.648	0.531	
ChargeO10		0.928	
Dipole	0.714	0.595	
EHOMO	-0.679	-0.644	

Extraction method: Principal Component Analysis.

Rotation Method: Varimax with Kaiser Normalization.

Rotation converged in 9 iterations.

Blank places are related to the data lower than 0.5 which were not selected

Table 6 has listed the variances explained by each principal component. As seen from this table, the first two principal components (PC1 and PC2) can explain more than 91% of variances in the original data matrix. To find a qualitative relationship between the resulted cyclic voltammograms and the structural features of Aq derivatives, the second score of the current data matrix was plotted against the first one in Figure 3. This figure shows that distinct clusters have been made by derivation which containing similar types of substituents. Each group was surrounded by an ellipse. The first class includes anthraquinones Aq1, Aq2, Aq3 and Aq4 have different substituents in position 1. The second class is related to Aq5 and Aq6 which have OH and NH_2 in position 2. Third class includes Aq7 and Aq8 which have two OH groups in position 1,4 and 1,8 that able to establishing stronger interamolecular hydrogen bond relative to others. Finally the forth class includes Aq9 and Aq10 which have two OCH_3 groups at position 1,4 and 1,8 as well as Aq3 which has one OCH_3 at position 1.

Table 6. Results of principal component analysis for molecular descriptors calculated by SPSS software

Total variance explained initial eigenvalues			
Component number	Total	% of Variance	Cumulative %
PC1	11.181	86.006	86.006
PC2	0.732	5.632	91.637
PC3	0.504	3.881	95.518
PC4	0.284	2.185	97.703
PC5	0.152	1.166	98.869
PC6	0.104	0.798	99.667
PC7	2.71×10^{-2}	0.208	99.876
PC8	9.63×10^{-3}	7.40×10^{-2}	99.95
PC9	6.56×10^{-3}	5.05×10^{-2}	100
PC10	1.33×10^{-15}	1.02×10^{-14}	100
PC11	1.93×10^{-16}	1.48×10^{-15}	100
PC12	-1.35×10^{-16}	-1.04×10^{-15}	100
PC13	-5.79×10^{-16}	-4.46×10^{-15}	100

Extraction Method: Principal Component Analysis.

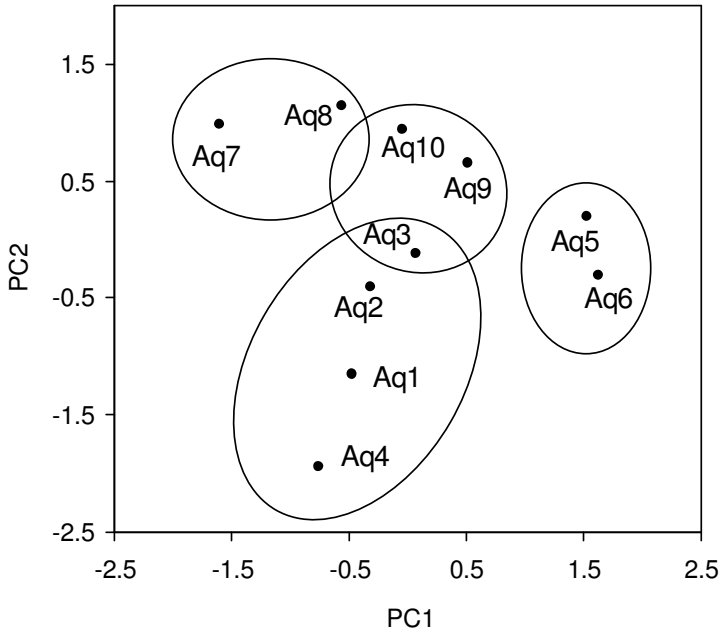

Figure 3. Score plot for classification of anthraquinone derivatives calculated by principal component analysis.

3.4. Solvent effect

3.4.1. Solvent parameters

The last row of Table1 contain the average values of experimental E_1^o, E_2^o in three solvents. Trends of average E_1^o and E_2^o values are; (E_1^o in AN) < (E_1^o in DMF) < (E_1^o in DMSO) and (E_2^o in AN)> (E_2^o in DMF) > (E_2^o in DMSO).

In order to evaluate these results better, solvent effects on the one-electron reduction potentials can be considered as a measure of the solvent dependence on the difference in the free energy of solvation for a redox couple [7];

$$\mathrm{Ox} + \mathrm{e}^- \rightleftharpoons \mathrm{Red}$$

$$E^{\circ} \approx IP - \frac{\Delta G^{\circ}_{\mathrm{solv}}(\mathrm{Red}) - \Delta G^{\circ}_{\mathrm{solv}}(\mathrm{Ox})}{F} + C \qquad (7b)$$

Where IP is the gas-phase ionization potential, C is the absolute potential of the reference electrode in a given solvent, $\Delta G°_{\mathrm{solv}}(\mathrm{Red})$ and $\Delta G°_{\mathrm{solv}}(\mathrm{Ox})$ are the free energies of solvation for the reduced and oxidized forms, respectively, and F is the Faraday constant. When the continuum model is used, the total free energy of solvation (ΔG_{solv}) is as following [35]:

$$\Delta G_{\mathrm{solv}} = \Delta G_{\mathrm{cav}} + \Delta G_{\mathrm{elst}} + \Delta G_{\mathrm{disp}} + \Delta G_{\mathrm{spec}} \qquad (8)$$

ΔG_{cav}, ΔG_{elst}, ΔG_{disp} and ΔG_{spec} characterize the contributions of cavity, electrostatic, dispersion and specific interactions of solute molecule with solvent, respectively. Therefore, with respect to Table 2, solvent effect can be interpreted based on the solvation free energy.

On the other hand, the cavity term depends on the size of solute and solvent molecule and dispersion contribution depends on polarizability, size, ionization potential of solute and solvent. Finally, electrostatic part correlates the polarity of solute and dielectric constant of solvent. Thus solvation can correlate size, polarizability and specific interaction such as hydrogen bond between solute and solvent. Therefore, solvent effect can be investigated by considering a few parameters of solvent without calculation of solvation free energy.

Modified Kamlet-Taft linear solvation free energy relationship [9] has been successfully applied to describe solvent effects as following:

$$E^{\circ\prime} = E^{\circ} + aV + b\delta_{\mathrm{d}} + c\delta_{\mathrm{h}} + d\beta + e\pi^* + f\varepsilon \qquad (9)$$

$E^{\circ\prime}$ is solvent dependent reduction potential and $E°$, a, b, c, d, e and f are solvent independent coefficients characteristic of the process, V is molar volume in $\mathrm{cm^3 mol^{-1}}$, δ_{d} is dispersion component of solubility parameters in $\mathrm{cal^{1/2} cm^{-3/2}}$, δ_{h} is hydrogen bonding component of solubility parameters in $\mathrm{cal^{1/2} cm^{-3/2}}$, β is the hydrogen bond acceptor or electron pair donor ability, π^* is its dipolarity/polarizability and ε is dielectric constant. The observed solvent effects were analyzed in view of the Kamlet-Taft relationship [21].

Since the number of solvents are limited in this study and are not enough for QSPR studies, then deriving a linear equation between experimental data for a few solvent properties is meaningless. Therefore, we focus ourselves on linear correlation between experimental voltammetry data and solvent parameters, individually. The solvent parameters, average values of E°_1, $E^{\circ}_1(\mathrm{ave})$, average

values of E_2^o, $E_2^o(\text{ave})$, and their correlation coefficients i.e. $R^2(E_1^o(\text{ave}))$, and $R^2(E_2^o(\text{ave}))$ are listed in Table 7. The $E_1^o(\text{ave})$ increases by increasing of size, dispersion, polarity, hydrogen bonding and dielectric constant of solvent, while $E_2^o(\text{ave})$ has inverse correlation with all of the parameters. Difference between these correlations is due to difference between interaction of solvent with neutral (Aq), radical anion ($Aq^{\cdot -}$) and dianion (Aq^{2-}) species.

Table 7. Average values of standard reduction potentials of Anthraquinones in different solvents accompanies to their solvent parameters and square of correlation coefficient (R^2).

Solvent	$E_1^o(\text{ave})$	$E_2^o(\text{ave})$	V	δ_d	δ_h	π^*	β	ε
AN	-0.889	-1.211	52.6	7.5	3.0	0.75	0.37	36.6
DMSO	-0.802	-1.314	71.3	9.0	5.0	1.00	0.76	47.2
DMF	-0.841	-1.256	77.0	8.5	5.5	0.88	0.69	38.2
$R^2(E_1^o(\text{ave}))$			0.596	0.983	0.630	0.999	0.915	0.816
$R^2(E_2^o(\text{ave}))$			-0.464	-0.933	-0.490	-0.991	-0.828	-0.907

δ_d and δ_h are in $cal^{1/2}cm^{-3/2}$, V is in cm^3/mol.
Average values and data parameters taken from Table 1 and Ref. 32, respectively

3.4.2. Explicit and implicit solvent effect

Figure 4 compares the solvent effect on E^o of each anthraquoinone derivative, individually. It shows variation of the first and second experimental reduction potential in different solvents with different dielectric constants. It is observed that E_1^o mostly increases with dielectric constant, while the E_2^o decreases with it. It can be related to different interactions between different forms (neutral, radical anion and dianion) of anthraquinones with solvent. These effects were appeared in the free energy of solvation and calculated reduction potential which tabulated in Tables 2 and 3. Calculated solvation energy by quantum mechanics considers implicitly different contributions such as electrostatic, dispersion, cavitation and repulsion. By comparing Fig 4a with figure 4c and Fig 4b with 4d, it is revealed that plot of experimental E_1^o, E_2^o versus dielectric constant is not similar to the plot of calculated quantum mechanical difference in free energy of solvation (Table 2) for the first and second steps, ($\Delta\Delta G_{solv}(1) = \Delta G_{solv}(A\dot{q}^-) - \Delta G_{solv}(Aq)$, $\Delta\Delta G_{solv}(2) = \Delta G_{solv}(Aq^{2-}) - \Delta G_{solv}(Aq)$, so they don't have good correlation. Because self consistent reaction field (SCRF) considers the solvent, implicitly, and can not clearly calculate solute-solvent and solvent-solvent interaction while explicit calculation can include them. So, when we compared experimental solvent effect and the results of calculated quantum mechanical solvent effect, the correlations were not acceptable (data not shown). Therefore we performed molecular mechanics using MM+ force field implemented in Hyperchem. In these calculations we considered 10 solvents molecules around the one molecule of anthraquinone and optimize the system of Aq derivatives in the presence of solvent molecules. Figure 5 shows distribution of solvent molecules around the Aq1 molecules in the neutral, radical anion and dianion

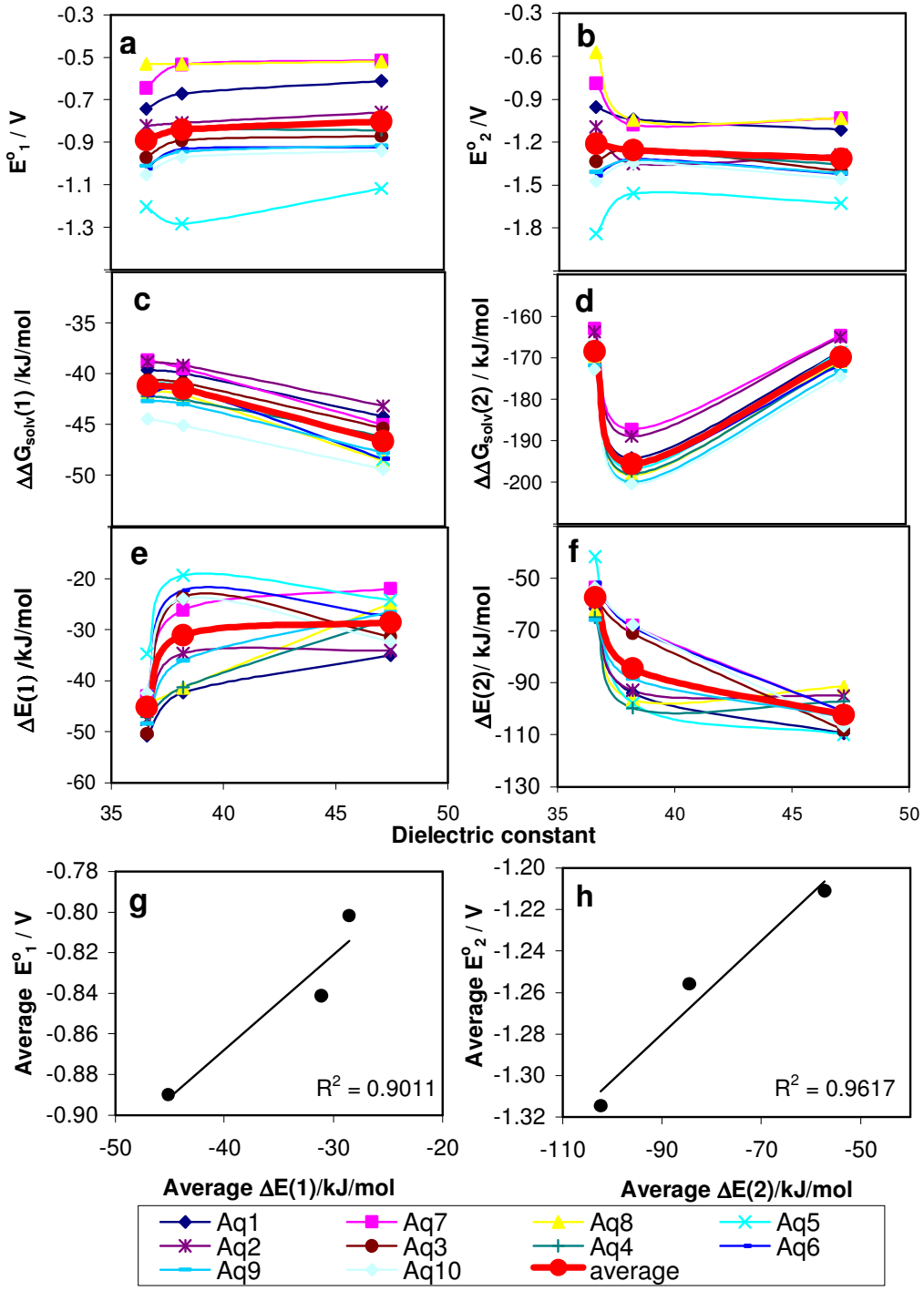

Figure 4. Variation of (a) experimental first reduction potential (E_1°), experimental second reduction potential (E_2°), (c) difference in free energy of solvation for the first step ($\Delta\Delta G_{solv}(1) = \Delta G_{solv}(A\dot{q}^{-}) - \Delta G_{solv}(Aq)$, (d) difference in free energy of solvation for the second step, $\Delta\Delta G_{solv}(2) = \Delta G_{solv}(Aq^{2-}) - \Delta G_{solv}(Aq)$ (e) difference in interaction energy for the first step ($\Delta E(1) = EA\dot{q}^{-} - EAq$), (f) difference in interaction energy for the second step ($\Delta E(2) = EAq^{2-} - EAq$) versus dielectric constant and (g) correlation between average experimental E_1° and average calculated interaction energy $\Delta E(1)$ (h) correlation between average experimental E_2° and average calculated interaction energy $\Delta E(2)$.

forms. In acetonitrile, by moving from neutral toward dianion form, the distribution seems to be more regular and hydrogen atom directed toward charged anthraquinone. While, that is less regular for other solvents, and seems that hydrogen also directs toward anthraquinone. In DMSO, sulfur atoms change direction toward charged anthraquinone. These changes may be due to more positive partial charge on hydrogen and sulfur atoms.

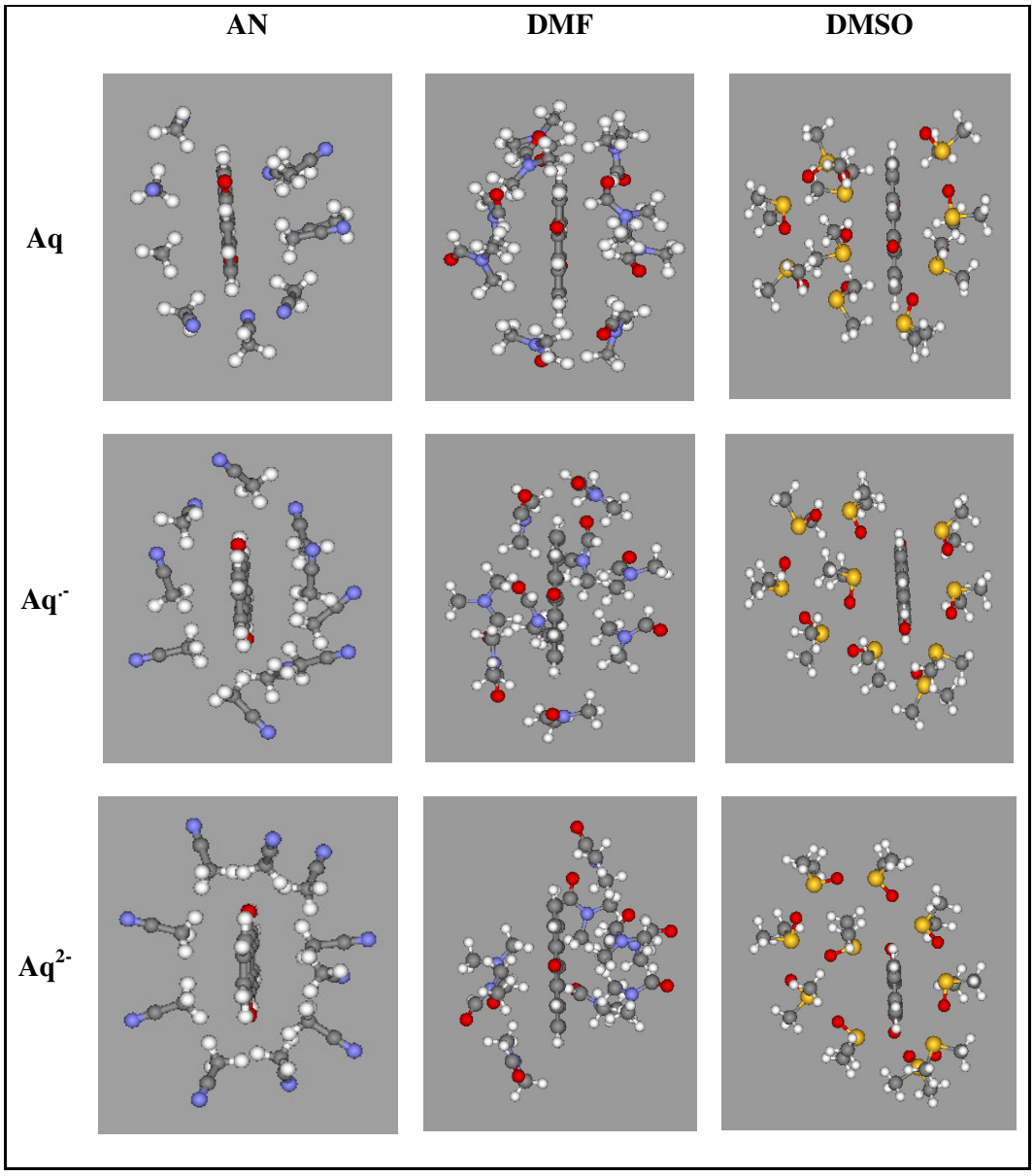

Figure 5. Distribution of solvent molecules around different forms of 9,10-anthraquinone (Aq1) calculated by molecular dynamics and MM^{+} force field, blue, white, dark, orange and red spheres represent the nitrogen, hydrogen, carbon, sulfur and oxygen, respectively.

When one compares figure 4a with 4e and Figure 4b with 4f, similar trend in reduction potential and difference interaction energy are observed. Figure 4g and 4h show correlation between E_1^o and E_2^o with difference in the interaction energies for the first ($\Delta E(1) = E\text{Aq}^{\cdot -} - E\text{Aq}$), and second step ($\Delta E(2) = E\text{Aq}^{2-} - E\text{Aq}$), respectively. It has better correlation, because of solvent-solvent interaction included in the calculation same as supermolecule methods. Thus, when we used explicit solvent effect molecular mechanics with MM^+ force field, we obtained more logical correlation (Figures. 4g and 4h).

4. CONCLUSIONS

Substituent and solvent effects on the electrochemical properties of some anthraquinone derivatives were studied by experimental and computational methods. Computational quantum mechanics and statistical methods calculated substituent and solvent effects in more detail by different descriptors and lead to the wide interpretation of substituent effects. Electrotoplogical descriptors, such as; charge, electron density, size and shape were found to be the best descriptors to representing solvent and substituent effects. It is concluded that $E°$ increases by increasing the hydrogen bonding, aromaticity and EHOMO and decreases by increasing size and polarity of anthraquinone. Variation of the first reduction potential with cited properties has reverse correlation with the second reduction potential. Namely, in the presence of solvent, the $E°$ values for the first reduction step increases with polarity, dielectric constant, molecular size and hydrogen bond of solvent, while this trend is reverse for the second step reduction potential. This is due to difference between solute-solvent interactions which discussed by explicit model better than continuum SCRF methods. Calculated quantum mechanics offers reasonable correlation with experimental results in each solvent. But, when we consider each anthraquinone in three solvents, SCRF could not present a good correlation with experimental values while molecular mechanics gives a better correlation.

ACKNOWLEDGMENT
Financial support of Damghan University of Basic Science is acknowledged. Dr Ghasem Aghapour for providing the compounds is also acknowledged.

References

1. R.H. Thomson, *Naturally Occurring Quinones*, Academic Press, New York, 1971.
2. M. Luckner, Secondary Metabolism in Microorganisms, Plants and Animals, Springer-Verlage. New York, 1984.
3. N.J. Low, R.E. Ashton, H. Koudsi, M. Verschoore, H. Schaefer*, J. Am. Acad. Dermatol.* 10 (1984) 69.
4. P.L. Gutierrez, B. Nguyen, In *Redox chemistry and interfacial behavior of biological molecules* (eds. G. Dryhurst and K. Niki) Plenum Press, New York, 1988.
5. G. Maia, F.C. Maschion, S.T. Tanimoto, K. Vaik, U. Mäeorg, K. *J. Solid State Electr.* 11 (2007) 1411.

6. D. Jeziorek, T. Ossowski, A. Liwo, D. Dyl, M. Nowacka, W. Woz´nicki, *J. Chem. Soc., Perkin Trans*. 2 (1997) 229.
7. R.M. Ion, F. Scarlat, V.I.R. Niculescu, *Rom. J. Phys.* 48 (2003) 1.
8. H. Svith, H. Jensen, J. Almstedt, P. Andersson, T. Lundbäck, K. Daasbjerg, M. Jonsson*, J. Phys. Chem. A* 108 (2004) 4805.
9. M. Jonsson, A. Houmam, G. Jocys, D. D.M. Wayner, *J. Chem. Soc., Perkin Trans 2* 2 (1999) 425.
10. M. Jonsson, D. Wayner, J. Lusztyk, *J. Phys. Chem.* 100 (1996) 17539.
11. S. Sinnecker, E. Reijerse, F. Neese, W. Lubitz, *J. Am. Chem. Soc.* 126 (2004) 3280.
12. C. Frontana, A. Va´zquez-Mayagoitia, J. Garza, R. Vargas, I. Gonza´lez, *J. Phys. Chem. A* 110 (2006) 9411.
13. (a) M.J. Kamlet, J.M. Abboud, M.H. Abraham, R.W. Taft, *J. Org. Chem.* 48 (1983) 2877.
14. S. Miertus, E. Scrorcco, J. Tomasi, *Chem. Phys.* 55 (1981) 117.
15. S. Miertus, J. Tomasi, *Chem. Phys.* 65 (1982) 239.
16. J. Tomasi, M. Persico, *Chem. Rev*. 94 (1994) 2027.
17. H.S. Rzepa, G.A. Suner, *J. Chem. Soc. Chem. Commun.* (1993) 1743.
18. M. Jalali-Heravi, M. Namazian, *J. Electroanal. Chem.* 425 (1997) 139.
19. C.A. Reynolds, *J. Am. Chem. Soc.* 112 (1990) 7545.
20. S.G. Lister C.A. Reynolds, W.G. Richards, *Int. J. Quantum Chem.* 41 (1992) 293.
21. K. Taras-Goslinska, M. Jonsson, *J. Phys. Chem. A* 110 (2006) 9513.
22. M. Shamsipur, A. Siroueinejad, B. Hemmateenejad, A. Abbaspour, H. Sharghi, K. Alizadeh, S. Arshadi, *J. Electroanal. Chem.* 600 (2007) 345.
23. S. Riahi, S. Eynollahi, M.R. Ganjali *Int. J. Electrochem. Sci.*, 4 (2009)1128.
24. A.J. Hamdan *Int. J. Electrochem. Sci.*, 5(2010)215.
25. P.S. Guin, S. Das, P. C. Mandal1, *Int. J. Electrochem. Sci.*, 3(2008)1016-1028 (PDF 321 K)
26. D. Ajloo, A.A. Saboury, N. Haghi-Asli, G. Ataie-Jafari, A.A. Mossavi-Movahedi, M. Ahmadi, K. Mahnam, S. Namaki, *J. Enz. Inhib. Med. Chem.* 22 (2007) 395.
27. D. Ajloo, A. Sharifian, H. Behniafar, *Bull. Korean Chem. Soc.* 29 (2008) 2009.
28. Gh. Aghapour, M.S Thesis，Shiraz Univercity, Shiraz, Iran, 1998.
29. J.J.P. Stewart, *J. Comput. Chem.* 10 (1989) 209.
30. M.J. Frisch, G.W. Trucks, H.B. Schlegel, G.E. Scuseria, M.A. Robb, J.R. Cheeseman, V.G. Zakrzewski, J.A. Montgomery Jr., R.E. Stratmann, J.C. Burant, S. Dapprich, J.M. Millam, A.D. Daniels, K.N. Kudin, M.C. Strain, O. Farkas, J. Tomasi, V. Barone, M. Cossi, R. Cammi, B. Mennucci, C. Pomelli, C. Adamo, S. Clifford, J. Ochterski, G.A. Petersson, P.Y. Ayala, Q. Cui, K. Morokuma, D.K. Malick, A.D. Rabuck, K. Raghavachari, J.B. Foresman, J. Cioslowski, J.V. Ortiz, B.B. Stefanov, G. Liu, A. Liashenko, P. Piskorz, I. Komaromi, R. Gomperts, R.L. Martin, D.J. Fox, T. Keith, M.A. Al-Laham, C.Y. Peng, A. Nanayakkara, C. Gonzalez, M. Challacombe, P.M.W. Gill, B. Johnson, W. Chen, M.W. Wong, J.L. Andres, C. Gonzalez, M. Head-Gordon, E.S. Replogle, J.A. Pople, GAUSSIAN98, Revision A.6, Gaussian Inc., Pittsburgh, PA, 1998.
31. P. Wignet, E.J. Weber, C.J. Cramer D.G. Truhlar, *Phys. Chem. Chem. Phys.* 2 (2000) 1231.
32. H. Reiss, A. Heller, *J. Phys. Chem.* 89 (1985) 4207.
33. G. Capranico, M. Binaschi, *Biochim. Biophys. Acta* 1400 (1998) 185.
34. K. Gunaydin, G. Topcu, R.M. Ion, *Nat Prod Lett.* 16 (2002) 65.
35. (a) I. Tvaroska, T. Kozar, *J. Am. Chem. Soc*. 102 (1980) 6929. (b) D.E. Leahy, *J. Pharm. Sci.* 75 (1986) 629.